0022-3565/09/3292-558–570$20.00
THE JOURNAL OF PHARMACOLOGY AND EXPERIMENTAL THERAPEUTICS
JPET 329:558–570, 2009

Vol. 329, No. 2
149831/3457017
Printed in U.S.A.

Expression Profiling of the Solute Carrier Gene Family in the Mouse Brain[S]

Amber Dahlin, Josh Royall, John G. Hohmann, and Joanne Wang

Department of Pharmaceutics, University of Washington, Seattle, Washington (A.D., J.W.); and Allen Institute for Brain Science, Seattle, Washington (J.R., J.G.H.)

Received December 13, 2008; accepted January 28, 2009

ABSTRACT

The solute carrier (Slc) superfamily is a major group of membrane transport proteins present in mammalian cells. Although Slc transporters play essential and diverse roles in the central nervous system, the localization and function of the vast majority of *Slc* genes in the mammalian brain are largely unknown. Using high-throughput in situ hybridization data generated by the Allen Brain Atlas, we systematically and quantitatively analyzed the spatial and cellular distribution of 307 *Slc* genes, which represent nearly 90% of presently known mouse *Slc* genes, in the adult C57BL/6J mouse brain. Our analysis showed that 252 (82%) of the 307 *Slc* genes are present in the brain, and a large proportion of these genes were detected at low to moderate expression levels. Evaluation of 20 anatomical brain subdivisions demonstrated a comparable level of *Slc* gene complexity but significant difference in transcript enrichment. The distribution of the expressed *Slc* genes was diverse, ranging from near-ubiquitous to highly localized. Functional annotation in 20 brain regions, including the blood-brain and blood-cerebral spinal fluid (CSF) barriers, suggests major roles of Slc transporters in supporting brain energy utilization, neurotransmission, nutrient supply, and CSF production. Furthermore, hierarchical cluster analysis revealed intricate *Slc* expression patterns associated with neuroanatomical organization. Our studies also revealed *Slc* genes present within defined brain microstructures and described the putative cell types expressing individual *Slc* genes. These results provide a useful resource for investigators to explore the roles of *Slc* genes in neurophysiological and pathological processes.

Transporters are integral membrane proteins whose primary function is to facilitate small molecule exchange across cell membranes. Because of its central role in neurotransmission and its high energy demand, the brain employs numerous membrane transport proteins to supply nutrients, facilitate energy production, control ion and pH balance, regulate neurotransmitter levels and activity, and remove metabolic byproducts (Blakely et al., 1994; Kusuhara and Sugiyama, 2004; Simpson et al., 2007). Many transporters, such as those within the solute carrier (SLC) 6 family of sodium and chloride-dependent neurotransmitter transporters, are involved in the genesis and development of brain disorders (Garland et al., 2002; Beart and O'Shea, 2007). Several transporters, such as the serotonin and norepinephrine reuptake transporters (SLC6A4 and SLC6A2, respectively) and the high-affinity glutamate transporters [e.g., excitatory amino acid transporter 2 (EAAT2)/SLC1A2], are important drug targets for the treatment of various psychiatric and neurological diseases (Torres et al., 2003; Rothstein et al., 2005). In addition, transporters expressed at the blood-brain interfaces, including the blood-brain barrier (BBB) and blood-cerebral spinal fluid barrier (BCSFB), are of great pharmaceutical importance because they are important determinants for drug disposition and targeting into the brain (Smith et al., 2004; Pardridge, 2007).

The SLC (or Slc) superfamily is a major group of membrane transport proteins that control cellular uptake and efflux of nutrients, neurotransmitters, metabolites, drugs, and toxins (Hediger et al., 2004). Approximately 360 *Slc* genes have been identified from the human and rodent genomes and assigned into 46 gene families (Hediger et al., 2004; refer to the HUGO Gene Nomenclature Committee Solute Carrier Family Series, http://www.bioparadigms.org/slc/menu.asp). Few of these transporters have been characterized fully in the central nervous system (CNS), and the biological and

This work was supported by the National Institutes of Health [Grants R01-GM066233, T32-GM007750].
Article, publication date, and citation information can be found at http://jpet.aspetjournals.org.
doi:10.1124/jpet.108.149831.
[S] The online version of this article (available at http://jpet.aspetjournals.org) contains supplemental material.

ABBREVIATIONS: Slc, solute carrier; EAAT, excitatory amino acid transporter 2; BBB, blood-brain barrier; BCSFB, blood-cerebrospinal fluid barrier; CNS, central nervous; ABA, Allen Brain Atlas; ISH, in situ hybridization; NCBI, National Center for Biotechnology Information; OATP, organic anion-transporting polypeptide; CLT, choline-like transporter; GLUT, glucose transporter; CSF, cerebrospinal fluid; UHCA, unsupervised hierarchical cluster analysis.

neurological functions of the vast majority of the *Slc* genes in the mammalian brain are largely unknown. In particular, the expression and distribution of most of the *Slc* genes in various brain microstructures and cell types have not been characterized. In addition, the physiological substrates of many Slc transporters in the brain remain unknown. Because specific physiological, behavioral, and higher order cognitive functions and many CNS disease processes are frequently associated with distinct brain regions and cell groups, deciphering the spatial and cellular expression patterns of *Slc* genes in the brain will provide crucial information regarding their neurophysiological and pathological functions in the CNS.

The Allen Brain Atlas (ABA) is a newly developed, genome-wide digital atlas of gene expression in the adult mouse brain (Bhattacharjee, 2006; Lein et al., 2007; Sunkin and Hohmann, 2007). Using highly standardized, automated high-throughput in situ hybridization (ISH) procedures, anatomically comprehensive expression patterns of over 16,000 genes were obtained at cellular resolution in the 56-day-old male C57BL/6J mouse brain (Lein et al., 2007). The primary goal of this study was to construct a comprehensive brain expression map for mouse *Slc* genes using high-quality ISH data generated by the ABA. Original ISH photomicrographs were manually analyzed for the expression of 307 *Slc* genes, corresponding to nearly 90% of all presently known mouse *Slc* genes, in 20 anatomically comprehensive brain areas, including two previously overlooked structures: the BBB and the BCSFB (i.e., choroid plexus). The putative cell types expressing each *Slc* gene were evaluated based on cell morphology and with reference to cellular marker genes. Unsupervised hierarchical cluster analysis was then employed to elucidate the distributional and potential functional relatedness of the *Slc* genes across the brain.

Materials and Methods

Databases and Analysis Tools. The primary database used in our study was the Allen Brain Atlas (http://www.brain-map.org). The construction and validation of the ABA was described previously (Lein et al., 2007). The NCBI databases (Genbank, UniGene), the Human Genome Organization Nomenclature Committee Database, the SLC genomic database at Bioparadigms, which includes more than 40 transporter families of the *Slc* gene series (available online at http://www.bioparadigms.org/slc/menu.asp) (Hediger et al., 2004), and PubMed were used to query individual *Slc* genes and to obtain information related to their substrates, tissue distribution, and other functions.

ISH Data Analysis. Image series from the Allen Brain Atlas were retrieved by entering the term "Slc" into the search function. Incomplete transcripts and pseudogenes were excluded from the data set. An initial search from the first ABA data release in 2006 returned ISH photomicrograph series for 298 *Slc* genes. Additional mouse *Slc* genes were further identified in GenBank, and corresponding probe sets were synthesized and utilized in automated high-throughput ISH at the Allen Institute for Brain Science. The ISH photomicrographs were visually inspected at multiple magnification levels. The sagittal image series near midline (lateral 0.5–1.5 mm) was primarily used for annotation, and when available, coronal sections were also evaluated for image and gene expression consistency. If apparent hybridization artifacts were seen, adjacent images or images from cross-sections were used for primary scoring. For each gene, expression density and level were subjectively scored with reference to the ABA expression heat mask in 20 anatomical subdivisions: olfactory bulb; cortex; striatum; pallidum; dentate gyrus; hippocampal fields CA1, CA2, and CA3; retrohippocampal formation; choroid plexus; thalamus; hypothalamus; superior and inferior colliculi (evaluated as one region); ventral tegmental area; substantia nigra; raphe nucleus; locus coeruleus; pons; medulla; and cerebellum. Brain microvessel expression was analyzed in regions enriched in vasculature, such as the thalamus, and expression level was semiquantitatively evaluated independently from the other brain regions.

Quantitative Analysis of *Slc* Gene Expression. Within a defined brain region, the tremendous cellular diversity and heterogeneity present a challenge for quantitative analysis of gene expression from histological ISH data. Previously, Lein et al. (2007) showed that relative density (D) and expression level (L) are the two most salient variables for quantitative analysis of brain ISH data. D is defined as the proportion of positively labeled cells in a defined area, and L is a measure correlated with the classic transcript intensity. The product, $D \times L$, was proposed as the metric to quantify gene expression in a defined area (Lein et al., 2007). The number of labeled cells in a defined brain structure was found previously to be the best predictor of whether or not a gene is considered to be "expressed" in that structure by colormetric ISH detection. A minimal cutoff of $>1.5\%$ of all 8×8-pixel regions containing segmented cell body was defined as the detection threshold (Lein et al., 2007). The same paradigm was used in our analysis. In brief, each ISH image was visually analyzed, and the numerical values for relative density (D, 0–4) and expression level (L, 0–5) were scored for each brain region with reference to the ABA expression heat mask. The D and L values were then multiplied to obtain the expression factor ($E = D \times L$). The mean and S.D. of the E values in the 20 individual brain regions were computed to obtain average expression factor ($\hat{E}$) for the whole brain. This average expression factor is a global assessment of transcript expression across the brain, whereas the S.D. reflects the degree of heterogeneous expression across the 20 anatomical regions. By definition, the upper limit of expression factor, in average or in individual areas, is 20, and the lower limit is 0. Based on the E value, five expression categories were assigned: "not detected" ($E = 0$), "low" ($0 < E < 4$), "moderate" ($4 \leq E < 10$), "intermediate to high" ($10 \leq E < 14$), and "very high" ($E \geq 14$). Putative cell type annotation of neurons, astrocytes, oligodendrocytes, brain microvessels, and choroid plexus epithelia was performed by morphological examination and by reference to cell type-specific markers, according to Lein et al. (2007).

Unsupervised Hierarchical Cluster Analysis. To investigate the potential anatomical and functional relationship of *Slc* gene expression in the brain, regional expression factor data were analyzed by unsupervised, two-way hierarchical cluster analysis using MATLAB R2007a software (Mathworks Inc., Natick, MA). Cluster analysis was first evaluated by running multiple combinations of distance and linkage models, and the quality of the various clustering solutions was then assessed by comparing the cophenetic distance coefficients for each model. It was found that the Euclidean distance followed by Ward's linkage (on the x-axis) and single linkage (on the y-axis) produced the highest cophenetic correlation coefficient (>0.9) and, therefore, was used in hierarchical cluster analysis. Because genes with uniform expression interfere with clustering and pattern identification, such genes, characterized by a S.D. of 0 for their average brain expression factor values, were filtered out of the data set, leaving a 235-gene matrix for analysis. The resulting cluster analysis was displayed as a graphic depicting a heat map of gene expression, flanked by dendrograms on the x and y axes.

Results

Global Expression of Slc Transcripts in the Mouse Brain. To identify *Slc* transporter genes analyzed by the ABA, the term "*Slc*" was used in the query function in the ABA. This search initially returned acceptable ISH data sets for 298 independent *Slc* genes. A family-based search in the

NCBI Genbank and UniGene databases further identified 29 putative mouse *Slc* genes, which were either not assayed by the ABA in their first data release or had failed ISH assay. Probe sets corresponding to these genes were synthesized and included in additional runs of automated high-throughput ISH at the Allen Institute for Brain Sciences. Of these probe sets, nine generated acceptable ISH data, whereas the remainder failed quality control. Therefore, the total number of *Slc* genes included in our final analysis was 307, which corresponds to 87% of the 351 full-length mouse *Slc* open reading frames existing in the NCBI database.

ISH data sets for each of the 307 *Slc* genes were retrieved and visually inspected in 20 brain anatomical subdivisions. For each gene, expression density (D) and level (L) were scored in individual brain areas, and the expression factor (E) in each area was calculated. The average expression factor ($\hat{E}$) across the brain was calculated as the mean of the E values from 20 individual areas. Based on the $\hat{E}$ values, the 307 analyzed *Slc* genes were classified into five categories. Approximately 18% of the 307 *Slc* genes had an $\hat{E}$ value of 0, and was considered not detected in the brain (Fig. 1a). Twenty-six percent of *Slc* genes was expressed at low levels ($0 < \hat{E} < 4$), and 43% was expressed at moderate levels ($4 \leq \hat{E} < 10$). Ten percent was expressed at intermediate to high levels ($10 \leq \hat{E} < 14$), and only 3% was expressed at very high levels ($\hat{E} \geq 14$) (Fig. 1a). Based on the known and proposed functions and substrates of human and rodent *Slc* genes, 46% of the 252 *Slc* genes present in the brain is involved in energy production and consumption, 14% is dedicated to neurotransmitter regulation, 10% mediates nutrient and ion balance, and 7% seems to play a role in cell growth and regulatory pathways (Fig. 1b). It is notable that approximately 23% of the *Slc* genes encodes orphan transporters with no identifiable substrates. The 252 *Slc* genes demonstrated a normal distribution of average expression factor values, but the resulting histogram

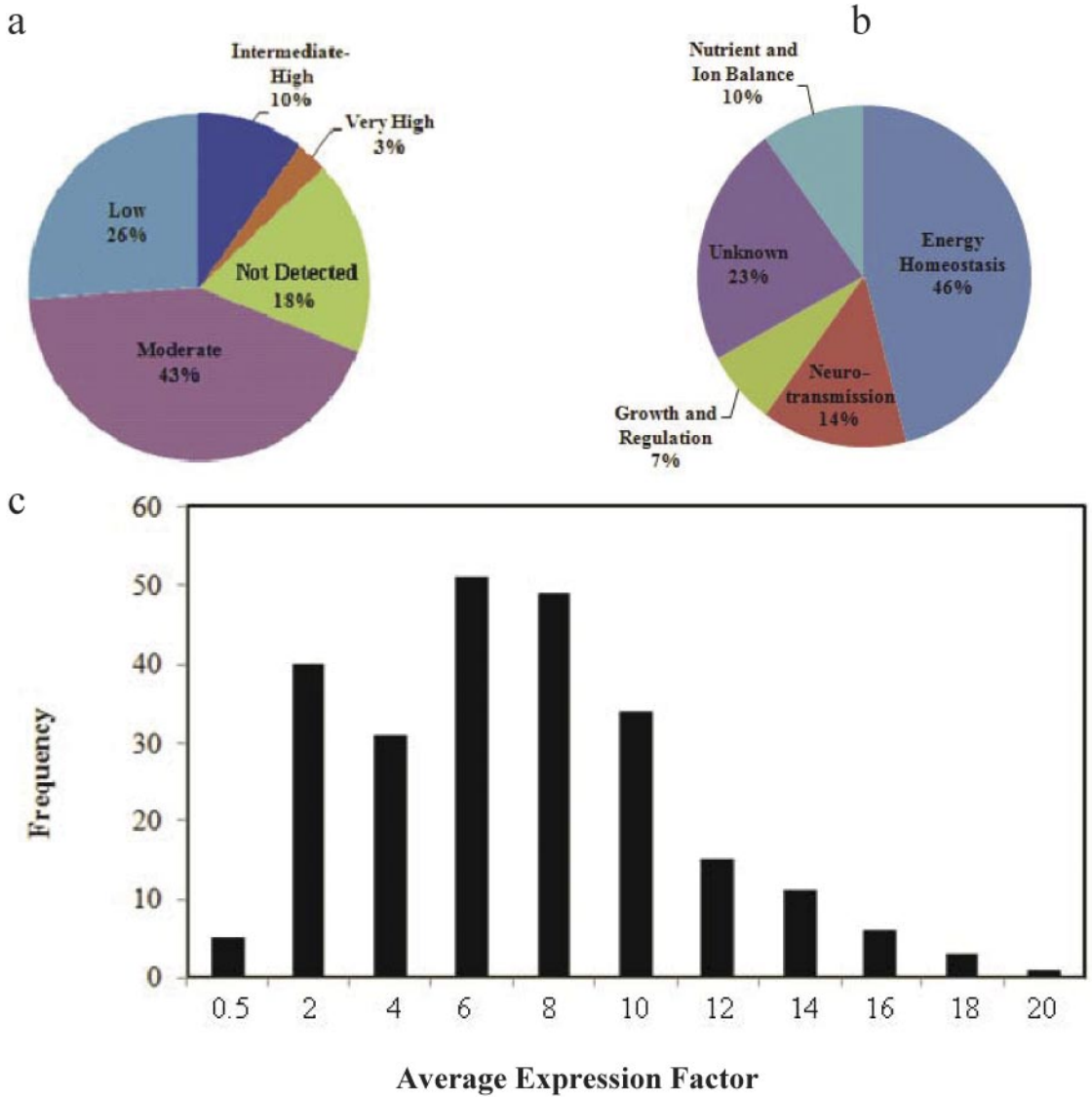

Fig. 1. Global expression of *Slc* transcripts in the mouse brain. a, pie chart shows the percentage of *Slc* genes in five expression categories based upon their average expression factor values ($\hat{E}$) across the brain. Based on $\hat{E}$ values, five expression categories were assigned: not detected ($\hat{E} = 0$), low ($0 < \hat{E} < 4$), moderate ($4 \leq \hat{E} < 10$), intermediate to high ($10 \leq \hat{E} < 14$), and very high ($E \geq 14$). b, pie chart displays the functional categories of *Slc* genes with detectable expression in the brain ($\hat{E} > 0$). c, histogram shows the distribution of average expression factor values of *Slc* genes expressed in the brain.

was slightly skewed leftward because of a significant representation of genes expressed at low to intermediate levels ($\hat{E}$ falling between 2 and 10 units) (Fig. 1c).

The 39 *Slc* genes with intermediate-high to very high average expression factor ($\hat{E} \geq 10$) in the brain are shown in Table 1. These genes, representing 20 different *Slc* families, are generally highly expressed and widely distributed in the brain. The *Slc25* family of mitochondrial carriers, the largest *Slc* family with at least 46 isoforms in man (Palmieri, 2004; Haitina et al., 2006), has nine isoforms represented in this category, accounting for nearly one quarter of the high expressers in the brain. Four of them (*Slc25a1*, *Slc25a4*, *Slc25a12*, *Slc25a23*) are expressed at the highest level ($\hat{E} \geq 14$), with a single isoform, the ADP/ATP carrier 1 (*AAC1*/*Slc25a4*), showing the highest $\hat{E}$ value ($\hat{E} = 20$) among all analyzed *Slc* genes. Other transporters that are highly expressed and widely distributed in the brain include transporters involved in nutrient (e.g., sugar, amino acids, fatty acids) transport, ion and pH balance, and trace metal (e.g., copper, zinc) homeostasis (Table 1). Several neurotransmitter transporters, including the EAAT2 (Slc1a2), a widely expressed glial transporter responsible for the majority of glutamate uptake in the brain (Kanai and Hediger, 2004; Tian et al., 2007), the plasma membrane monoamine transporter (Slc29a4), a newly identified brain biogenic amine transporter (Engel et al., 2004; Dahlin et al., 2007), the GABA transporter 3 (Slc6a11), and the vesicular glutamate transporter 1 (Slc17a7), are also associated with high $\hat{E}$ values. Several *Slc* genes in this high expression/wide distribution category are orphan transporters whose substrates have not been identified yet (Table 1).

Among the 307 *Slc* genes analyzed, 55 showed ISH signals not significantly above background in all 20 brain regions ($\hat{E} = 0$) and were classified as not detected in the brain (Supplemental Table 1). A number of these transporters, such as the Na^+-taurocholate-cotransporting polypeptide (Slc10a1), the organic anion-transporting polypeptide 1a1 (OATP1a1/Slco1a1), and the urate transporter 1 (Slc22a12), are known to be expressed in a tissue-specific manner in liver and/or kidney, where they mediate the excretion or reabsorption of circulating metabolites (e.g., bile acids, bile salts, urate, etc.) (Hagenbuch and Meier, 1994, 2004; Enomoto et al., 2002). Many others genes not detected in the brain seem to have equivalent isoforms that transport similar categories of substrates in the brain (Table 1; Supplemental Table 1). One gene, Slc1a7 (EAAT5), is exclusively expressed in the retina (Arriza et al., 1997), an area not included in the ABA ISH assay.

Gene Expression Patterns and Regional Enrichment. To investigate the regional distribution of *Slc* genes across the brain, the number of genes present in a specific anatomical region was determined, and the percentage of

TABLE 1
Slc genes with high average expression factor values ($\hat{E} \geq 10$) in the brain

Gene Symbol	Protein Name	Substrates	Average Expression Factor
Slc1a2	EAAT2	L-Glutamate, D-/L-aspartate	11.38
Slc2a12	GLUT12	Glucose	10.71
Slc6a11	GAT3	GABA	10.33
Slc6a17	NTT4	Unknown	13.86
Slc7a4		Arginine, lysine, and ornithine	11.19
Slc7a6	y^+LAT2	Cationic and large neutral L-amino acids	13.48
Slc8a1	NCX1	Na^+, Ca^{2+}	10.14
Slc8a2	NCX2	Na^+, Ca^{2+}	10.81
Slc9a1	NHE1	Na^+, H^+, Li^+, NH_4^+	11.43
Slc9a3r1	NHERF	NHE3-regulatory factor	12.90
Slc9a7	NHE7	Na^+, K^+, H^+, Li^+	12.52
Slc12a5	KCC2	K^+, Cl^-	10.90
Slc17a7	VGLUT1	Glutamate	10.05
Slc22a7	OAT2	Organic anions, polyspecific	12.90
Slc22a17	BOIT	Unknown	16.05
Slc23a2	SVCT2	L-Ascorbic acid	10.05
Slc24a2	NCKX2	Na^+, Ca^{2+}, K^+	15.33
Slc24a3	NCKX3	Na^+, Ca^{2+}, K^+	13.90
Slc25a1	CIC	Citrate, malate, PEP	15.19
Slc25a3	PiC	Phosphate	11.76
Slc25a4	AAC1	ADP, ATP	20.00
Slc25a5	AAC2	ADP, ATP	12.43
Slc25a11	OGC	Oxoglutarate, malate	12.00
Slc25a12	AGC1	Aspartate, glutamate	17.24
Slc25a23	APC2	ATP, ADP, AMP, and Pi	14.24
Slc25a27	UCP4	H^+	13.62
Slc25a36		Unknown	13.90
Slc27a1	FATP1	Long-chain fatty acids	10.71
Slc29a3	ENT3	Purine and pyrimidine nucleosides, nucleobases	10.05
Slc29a4	PMAT	Biogenic amines, adenosine	10.48
Slc30a2	ZNT2	Zinc	16.57
Slc30a9	ZNT9	Unknown	10.00
Slc31a2	Ctr2	Copper	11.10
Slc35a1	CST	CMP-sialic acid	14.52
Slc35b4		Unknown	12.90
Slc38a2	SNAT2	Alanine, asparagine, cysteine, glutamine, glycine, histidine, methionine, proline, serine	12.62
Slc39a7	KE4	Manganese	12.29
Slc43a2	LAT4	Neutral amino acids	10.29
Slc43a3	EEG1	Unknown	11.00

these genes in each expression factor category was calculated (Fig. 2). In terms of gene diversity (i.e., gene numbers), all regions, with the exception of the choroid plexus, exhibited a similar level of complexity, expressing 223 to 233 different *Slc* genes (mean, 226 ± 6), corresponding to ~90% of the 252 *Slc* genes present in the brain. The choroid plexus contained slightly fewer genes (202 genes). No single brain region expressed all 252 genes. With respect to expression factor, significant regional differences were observed. In structures containing dense populations of cell bodies relative to nerve terminals, such as the hippocampal areas (dentate gyrus and fields CA1, CA2, and CA3), cerebellum, and olfactory bulb, a larger proportion of *Slc* genes (>20%) was observed at high expression levels ($E \geq 10$). Other regions contained a smaller percentage of highly expressed *Slc* genes. For example, within the pallidum, which is densely innervated by neural processes and contains fewer cell bodies, the smallest fraction (8%) of highly expressed *Slc* genes was found (Fig. 2).

The 252 *Slc* genes present in the brain revealed diverse expression patterns. The vast majority of *Slc* genes showed heterogeneous expression; of these, many were enriched in distinct brain regions. In contrast, a small number of *Slc* genes were uniformly or near uniformly expressed in the brain. Figure 3 provides visual illustrations of *Slc* genes that are either ubiquitously distributed or regionally enriched in the cerebral cortex, striatum, and brain stem. A number of *Slc* genes were highly localized to specific fine structures (Fig. 4). These include known highly localized genes, such as the dopamine transporter (*DAT*/*Slc6a3*) in the substantia nigra and ventral tegmental area (Torres et al., 2003), the serotonin transporter (*SERT*/*Slc6a4*) in the median and dorsal raphe nuclei (Blakely et al., 1994), *EAAT4* (*Slc1a6*) in the Purkinje cell layer of the cerebellum (Kanai and Hediger, 2004), and the anion exchanger 2 (*AE2*/*Slc4a2*) in the choroid plexus (Lindsey et al., 1990) (Fig. 4). Highly localized or uniquely enriched patterns were revealed for the first time for a number of other *Slc* genes. For example, we found that the anion exchanger gene *Slc26a4* (*pendrin*), which is mutated in congenital sensorineural deafness and thyroid goiter (Pendred syndrome) (Scott et al., 1999), is present in the brain and highly enriched in the hippocampal areas (dentate gyrus, CAI-III) (Fig. 4a). In addition, *Slc39a6* (*Liv-1*), a newly described zinc transporter first identified as an estrogen-regulated gene in breast cancer (Taylor et al., 2007), is highly localized to the dentate gyrus of the hippocampus, with minimal presence in CA fields or other brain areas (Fig. 4b). The newly discovered plasma membrane monoamine transporter (*Slc29a4*) is particularly enriched in the dentate gyrus and choroid plexus (Fig. 4c). The equilibrative nucleoside transporter 1 (*Slc29a1*), the principal adenosine uptake transporter (Kong et al., 2004), is uniquely enriched in the thalamus (Fig. 4d). The gene encoding Slc26a11, a putative sulfate transporter, is highly localized to the choroid plexus (Fig. 4e). The vesicular glutamate transporter 3 (*Slc17a8*) is highly localized to the dorsal and medial raphe nuclei (Fig. 4g). The highly localized expression patterns of these genes may suggest novel and specialized functions of these transporters in the neurochemical

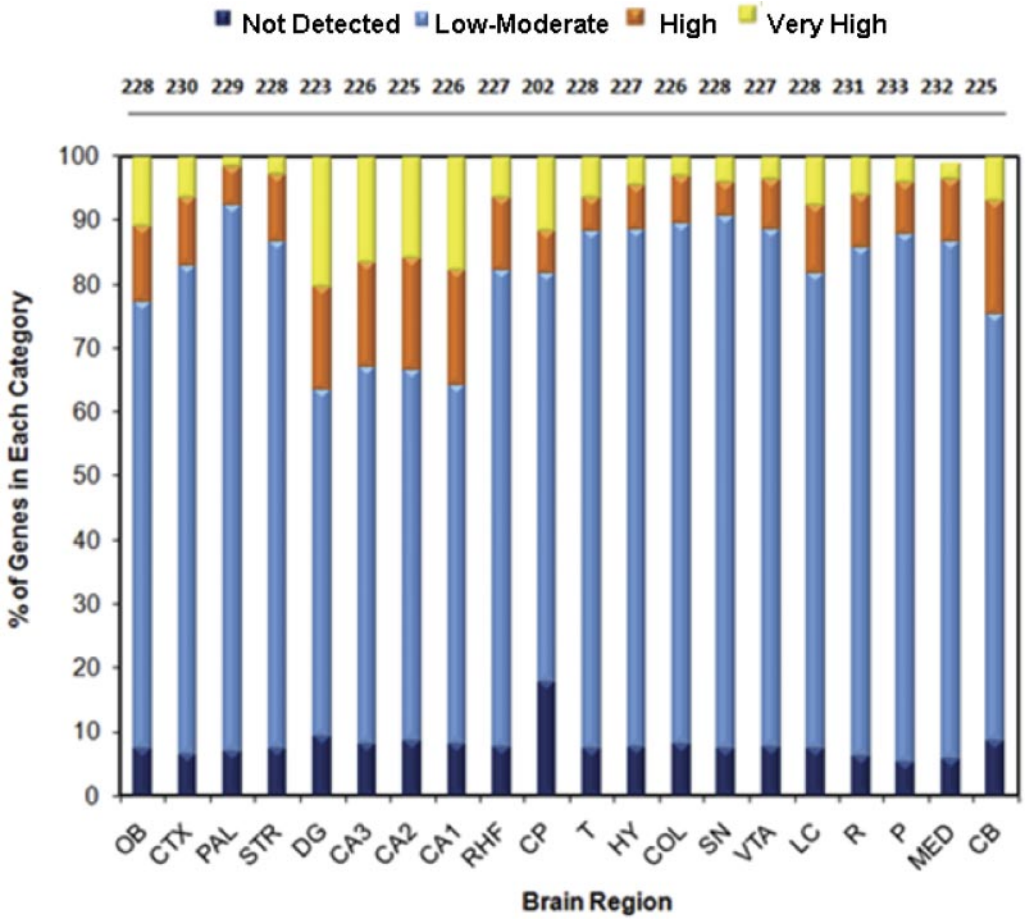

Fig. 2. Gene diversity and distribution of expression factor in individual brain regions. The numbers above each bar indicate the total number of genes present ($E > 0$) in the corresponding brain region. The percentage of *Slc* genes within each expression factor category, indicated by color-coded bars [dark blue, not detected ($E = 0$); light blue, low to moderate ($0 < E \leq 9$); orange, intermediate to high ($9 < E \leq 13$); yellow, very high ($13 < E \leq 20$)] for each brain area is shown on the *y*-axis. Labels on *x*-axis correspond to brain regions: OB, olfactory bulb; CTX, cerebral cortex; PAL, pallidum; STR, striatum; DG, dentate gyrus; CA3, CA3 hippocampal field; CA2, CA2 hippocampal field; CA1, CA1 hippocampal field; RHF, retrohippocampal formation; CP, choroid plexus; T, thalamus; HY, hypothalamus; COL, colliculi; SN, substantia nigra; VTA, ventral tegmental area; LC, locus coeruleus; R, raphe; P, pons; MED, medulla; and CB, cerebellum.

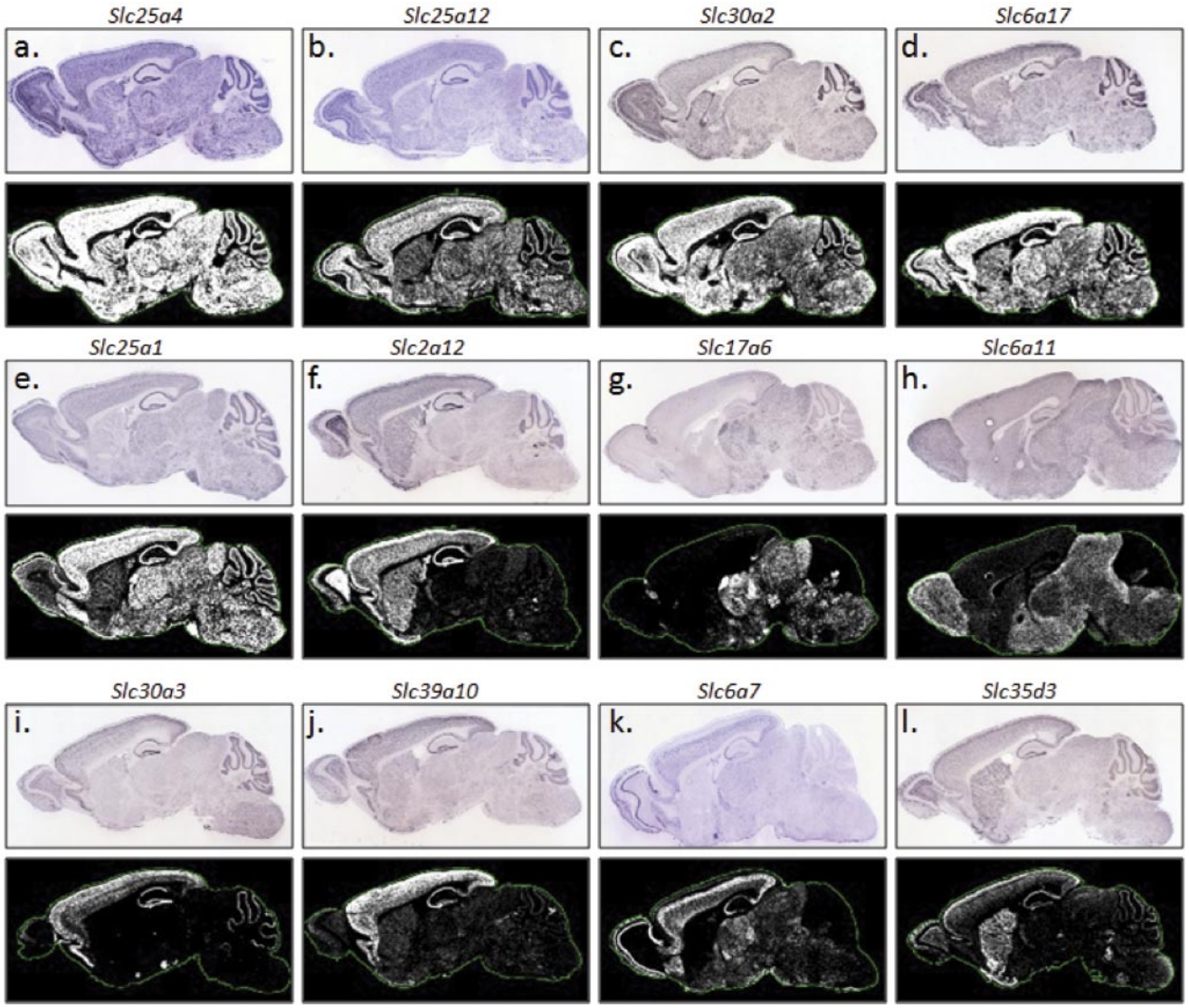

Fig. 3. Examples of expression patterns for ubiquitously and regionally expressed *Slc* genes. a through e, typical ISH results for ubiquitously and near-ubiquitously expressed genes. Regionally localized *Slc* genes are shown in f through l. Genes enriched in the cortex are shown in i through l. For each gene, the top represents the ISH image, and the bottom is the expression mask generated from the ISH image.

network. Based upon the specificity of their cellular expression and fine structure distribution, these *Slc* genes may also serve as potential markers for specific cell groups and microstructures.

Enriched Expression in Major Cell Types. The expression of *Slc* genes in major brain cell types is largely unknown. The fine resolution achieved by the ABA ISH data permits expression analysis at the cellular level. Thus, an important goal of this study was to evaluate the putative cell types of *Slc* expression in neurons, astrocytes, oligodendrocytes, choroid plexus epithelia, and microvessel endothelia. The putative cell types expressing individual *Slc* genes are summarized in Supplemental Figs. 1 to 4. Figures 5 and 6 provide examples of the observed cellular expression patterns for selected *Slc* genes. Brain sections showing distinct expression patterns for established cellular markers of neurons (*Mtap2*), interneurons (*Chat*), astrocytes (*Gja1*), oligodendrocytes (*Mopb*), choroid plexus epithelia (*Ace*) and brain microvessels (*Vwf*) were used as references for comparison (Figs. 5 and 6). In general, most *Slc* genes seem to have neuronal or mixed cellular expression patterns. Many *Slc* genes showed distinctly neuronal expression (e.g., *Slc1a1* and *Slc25a14* in Fig. 5, b–c), of which some were clearly present in interneurons (e.g., *Slc5a7* and *Slc17a8* in Fig. 5, e–f). A number of genes, such as *Slc6a11* (Fig. 5h), *Slc1a2*, and *Slc1a3* (Fig. 5i), demonstrated enriched expression in cells that are morphologically similar to astrocytes. A small number of genes, including the choline transporter-like protein 1 (*CLT1*/*Slc44a1*), were present in oligodendrocytes as demonstrated by their characteristic distribution in the white matter (e.g., corpus callosum) and by similarity to the distribution pattern of *Mopb*, an oligodendrocyte-specific gene marker (Fig. 6, a–c).

Expression at the Blood-Brain Barrier. Transporters at the BBB are thought to play central roles in supplying vital nutrients to neurons and other cells within the brain (Allen and Geldenhuys, 2006; Simpson et al., 2007). Here, we semiquantitatively analyzed *Slc* gene expression in brain microvessels by morphology and in reference to the blood vessel endothelial cell marker, *Vwf* (Fig. 6g). Distinct mi-

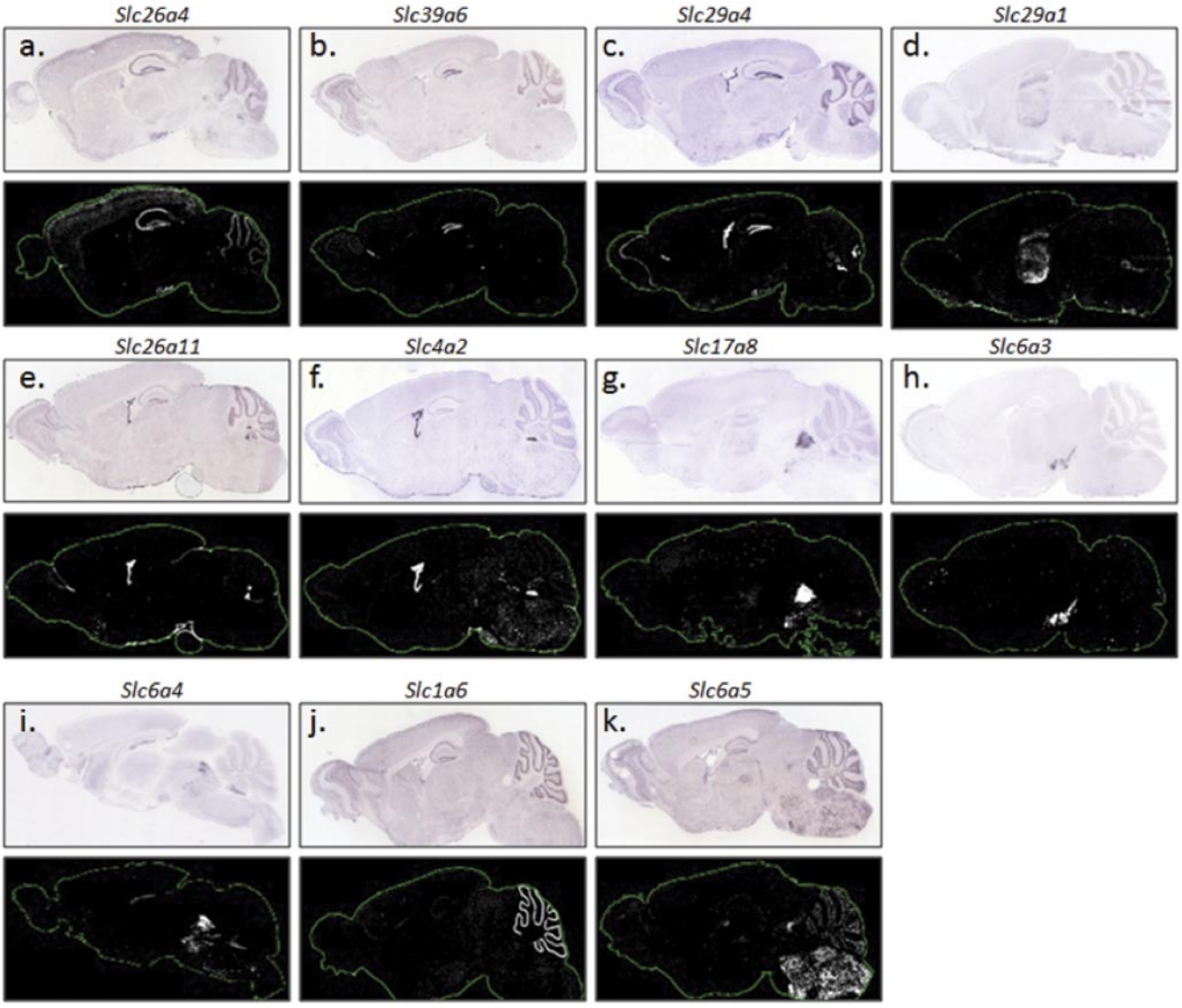

Fig. 4. Expression patterns observed for some highly localized *Slc* genes. In the forebrain, genes that are highly localized in the hippocampal formation, dentate gyrus and thalami are shown in a through d. e and f, choroid plexus-enriched genes. *Slc* genes that were highly localized to the midbrain (g–i), cerebellum (j), and medulla (k) were also observed. For each gene, the top represents the ISH image, and the bottom is the expression mask generated from the ISH image.

crovessel expression patterns are apparent for 36 *Slc* genes, and examples of typically observed BBB expression patterns are shown in Fig. 6, h and i. The 36 *Slc* genes include transcripts not previously observed in the BBB in addition to well characterized BBB genes such as *GLUT1* (*Slc2a1*), *Oatp1c1* (*Slco1c1*), *LAT1* (*Slc7a5*), and *OAT3* (*Slc22a8*) (Lee et al., 2001; Li et al., 2001; Enerson and Drewes, 2006). These genes, their transported substrates, relative expression levels at the BBB, and average brain expression factor values were summarized in Table 2. Consistent with the role of the BBB in supplying essential nutrients to the brain, we found that 25 of the 36 (~70%) *Slc* genes present at the BBB are engaged in the transport of nutrients or nutrient supplements, including transporters for simple sugars (*Slc2a1*, *Slc2a5*, *Slc2a10*, *Slc2a13*); amino acids (*Slc1a2*, *Slc3a1*, *Slc7a5*, *Slc6a6*, *Slc6a20*, *Slc7a11*, *Slc38a3*, *Slc38a5*); oligopeptides (*Slc15a2*, *Slc15a3*); long-chain fatty acids (*Slc27a5*); mono-, di-, and tricarboxylates (*Slc13a3*, *Slc13a5*, *Slc16a1*); folates/thiamines (*Slc19a1, Slc19a2*); L-ascorbic acids (*Slc23a1*, *Slc23a2*); carnitine (*Slc22a5*); and thyroid hormones (*Slc16a2*, *Slco1c1*). Other *Slc* genes found at the BBB include a urea transporter (*Slc14a1*) and five polyspecific organic cation or anion transporters (*Slco1a4*, *Slco1a6*, *Slc22a3*, *Slc22a7*, *Slc22a8*), which may mediate the efflux of various metabolic waste products from the brain. The remaining BBB-expressed genes include two trace metal transporters (*Slc11a2*, *Slc30a1*), a phosphate transporter (*Slc20a2*), a sulfate transporter (*Slc13a4*), and a scaffold protein (*Slc9a3r2*). The majority of genes present in brain microvessels were also expressed at low to moderate levels in other brain regions (between 2 and 10 units). However, several genes, including the facilitative glucose transporters 1, 5, and 10 (*GLUT1*/*Slc2a1*, *GLUT5*/*Slc2a5*, *GLUT10*/*Slc2a10*), the Na^+-imino acid transporter (*Slc6a20*), the cystine/glutamate exchanger (*Slc7a11*), the sodium-dicarboxylate cotransporter 2 (*Slc13a3*), and OATP1a6 (*Slco1a6*), are specifically enriched at the BBB because they showed zero or very low average brain expression factor values (Table 2).

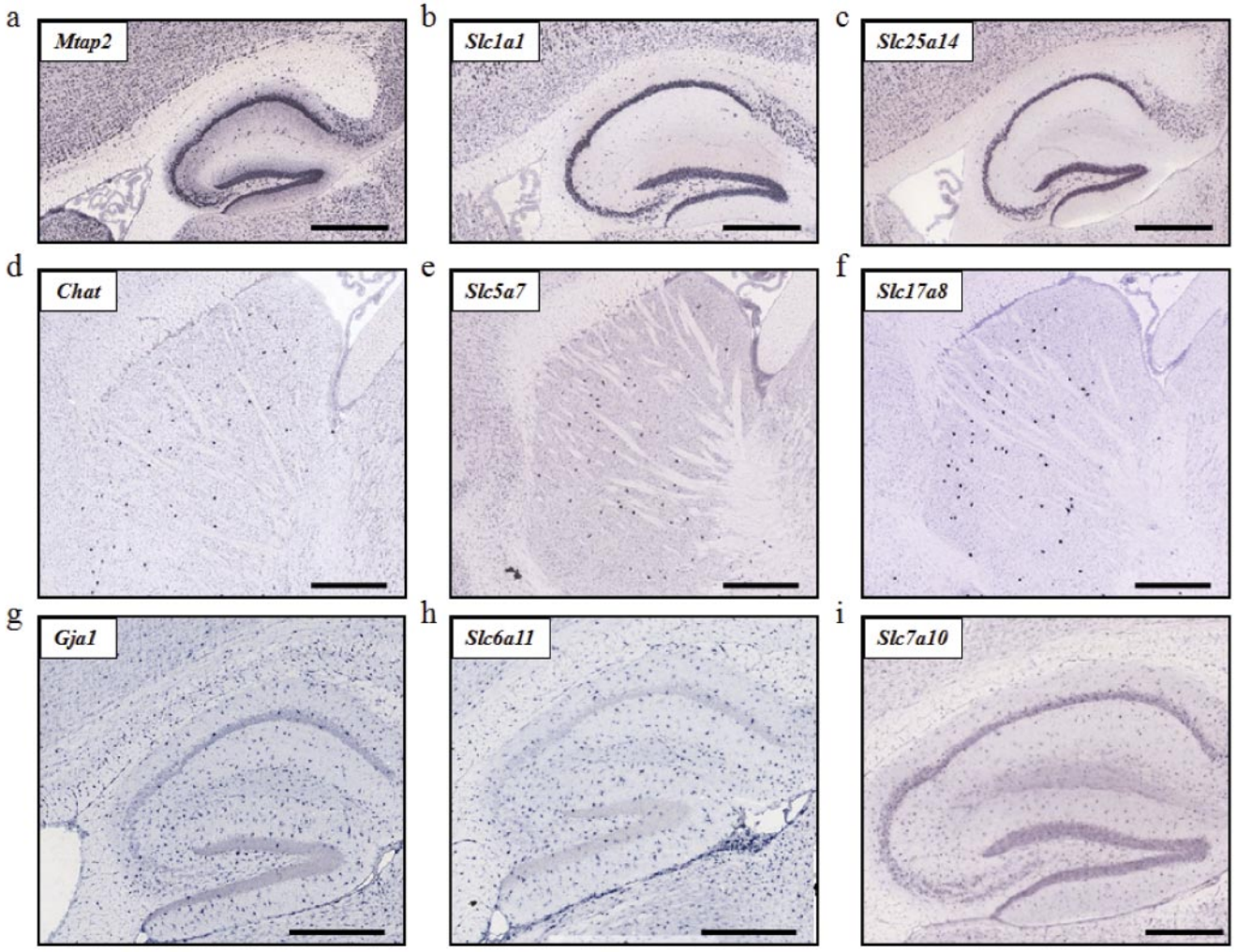

Fig. 5. Cellular expression patterns of *Slc* genes within neurons and astrocytes. Neuron-specific marker *Mtap2* (shown in a) was used as a reference for genes with neuronal expression patterns [e.g., *Slc1a1* (b) and *Slc25a14* (c) in the hippocampus]. The interneuron-restricted *Chat* [expressed in striatal interneurons in (d)] was used as a marker for genes with interneuron expression [*Slc5a7* (e) and *Slc17a8* (f) in the striatum]. In h and i, *Slc* transporters demonstrate cellular expression patterns similar to that of the astrocyte marker, *Gja1* (g).

Expression at the Blood-CSF Barrier. The choroid plexus epithelial cells in the brain ventricles form the second largest brain-blood interface, the BCSFB. A major function of the choroid plexus is to secret CSF, which is accomplished by active transport of small ions (e.g., Na^+, Cl^-, bicarbonate) across the choroidal epithelium. Besides CSF production, the choroid plexus may also supply the brain with certain nutrients, hormones, and metal ions and remove metabolites and toxins from the CSF (Miller, 2004; Smith et al., 2004). By annotation, 202 *Slc* genes were found in the choroid plexus (Fig. 2). The majority (~80%) of the *Slc* genes in the choroid plexus are expressed at low to moderate levels, whereas 27 *Slc* genes are expressed at the highest levels, with $E \geq 16$ (Table 3). These highly expressed genes include several electrolyte transporters involved in CSF secretion, such as *NKCC1* (*Slc12a2*), *AE2* (*Slc4a2*), and *NCBE* (*Slc4a10*). The *Slc25* family of mitochondrial carriers was also well represented, with six isoforms highly expressed in the choroid plexus. This observation is consistent with mitochondrial enrichment and high Na^+/K^+ ATPase activity in the choroid plexus, which provides the ion gradient and driving force for CSF production (Smith et al., 2004). Other highly expressed *Slc* genes include transporters for nutrients, thyroid hormones, sulfate, and trace metals. Most transporters expressed in the choroid plexus were coexpressed in other brain regions and cell types; however, a very small number of genes, e.g., the sodium-independent sulfate transporter *Slc26a11* (Fig. 6e; Table 3), seemed to be expressed only in the choroidal epithelia. Although *Slc26a11* is reportedly expressed at high levels in the placenta, kidney, brain, and high endothelial venules (Vincourt et al., 2003), this is the first report of its localization to a specific brain structure. The role of *Slc26a11* in the choroid plexus epithelia is presently unknown but may be potentially related to sulfate utilization in the brain.

Clustering of Correlated Gene Expression. To explore potential functional relatedness of the *Slc* genes and possible anatomic association with brain microstructures, we implemented unsupervised, two-way hierarchical cluster analysis to reveal the expression patterns of *Slc* genes in 20 brain regions. The results of this analysis are shown in Fig. 7. On the *x*-axis, the resulting dendrogram ordered the 20 evaluated brain regions into two major clusters, with the choroid plexus comprising a third cluster. The other 19 brain areas were ordered into several branches and subbranches within

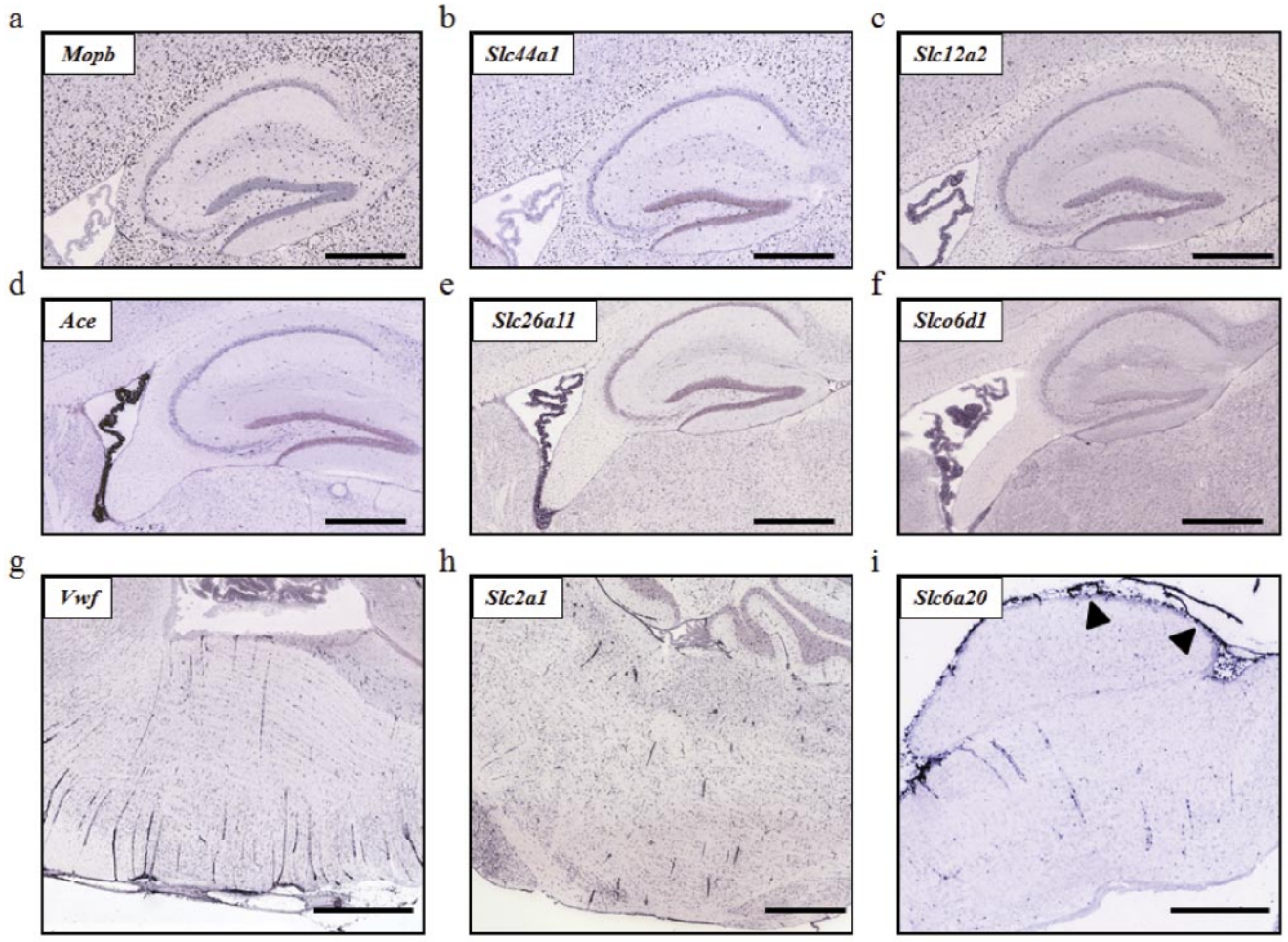

Fig. 6. Cellular expression patterns of *Slc* genes within oligodendrocytes, choroid plexus epithelia, and brain microvessel endothelial cells. Cell type-specific markers for oligodendrocytes (a), choroid plexus epithelia (d), and brain microvessel endothelia (g) were used to distinguish the cellular expression patterns of *Slc* genes. Examples of *Slc* genes expressed in oligodendrocytes (b and c), choroid plexus (e and f), and brain microvessel (h and i) and pia mater membrane [darts (i)] are shown.

the two dominant clusters. Anatomically proximal regions were closely coclustered (Fig. 7b), illustrating that functionally and anatomically related structures share a higher degree of overlapping *Slc* expression profiles.

The resulting *y*-axis dendrogram consisted of two major branches (Fig. 7). The upper branch (cluster I) contained the low- and variable-expression factor clusters, whereas the lower branch (cluster II) included the high expression factor clusters. Cluster I was further divided into subclusters, IA and IB. Cluster IA contained *Slc* genes that tended to have a localized distribution pattern (Supplemental Fig. 1). A group of these genes, including *Slc39a12*, *Slc24a5*, *Slco6d1*, and *Slc26a11*, were highly expressed and localized in the choroid plexus. Another group of genes, including *Slc41a3*, *Slco4a1*, and *Slc9a3*, were highly enriched in the cerebellum. Cluster IB, the largest subcluster, contained genes that were characterized generally by wide distribution and low to moderate expression factor values (Supplemental Fig. 2). However, a minority of cluster IB genes were highly localized. Genes in the second major branch, cluster II, possessed two consistent traits: widespread distribution and intermediate to high levels of expression in multiple regions (Fig. 7). Another interesting observation of cluster II was the marked enrichment of *Slc* genes in the hippocampal areas (Fig. 7). Within cluster II, three subbranches, IIA, IIB, and IIC, were present. Cluster IIA contained genes that seem to be high expressers in choroid plexus, but are also highly expressed in a few other areas including the hippocampus (Supplemental Fig. 3). The smallest subbranch, cluster IIB, contained only 11 genes, which generally demonstrated high expression in nearly all brain regions but were low or not detected in the choroid plexus (Supplemental Fig. 3). Cluster IIC, the largest subbranch in cluster II, contained genes that showed variable expression across the brain but were particularly enriched in the hippocampal region. Like cluster IIB, genes in cluster IIC were also absent or expressed at low levels in the choroid plexus (Supplemental Fig. 4).

Discussion

In this study, we comprehensively and systematically analyzed the expression patterns of 307 *Slc* genes, representing nearly 90% of presently known mouse *Slc* genes, in the mouse brain. To our knowledge, this is the first study in which a detailed expression analysis was performed for a single gene superfamily in the mammalian brain. This is also the first study in which mammalian *Slc* genes were comprehensively characterized in a distinct organ structure.

TABLE 2
Slc genes that are significantly expressed in the BBB

Gene Symbol	Protein Name	Substrates	Relative BBB Expression Level[a]	Average Expression Factor in Brain
Slc1a2	GLT-1 EAAT2	L-Glu, D-/L-Asp	+	11.38
Slc2a1	GLUT1	Glucose, galactose, mannose, glucosamine	+++	0
Slc2a5	GLUT5	Fructose	++	1
Slc2a10	GLUT10	Glucose, galactose	+	1
Slc2a13	HMIT	*Myo*-inositol	+	8.9
Slc3a1	rBAT	Slc7a9 heavy subunit	+	7.43
Slc6a6	TAUT	Taurine	++	6.81
Slc6a20	SIT1	Imino acids	+++	4.33
Slc7a5	LAT1	Large neutral amino acids, T3, T4, L-dopa	+	6.52
Slc7a11	xCT	Cystine, L-glutamine	+++	0.57
Slc9a3r2	NHERF-2	NHE3	+	9.38
Slc11a2	DMT1	Fe^{2+}, Cd^{2+}, Co^{2+}, Cu^{1+}, Mn^{2+}	+	3.67
Slc13a3	NaC2 SDCT2	Succinate, citrate, α-ketoglutarate	++	0.1
Slc13a4	NaS2	Sulfate	+	7
Slc13a5	NaC3	Citrate	+	2.38
Slc14a1	UT-B1	Urea	+	5.19
Slc15a2	PEPT2	Di- and tripeptides	+	4.19
Slc15a3	PHT2	Histidine and di- and tripeptides	+	2.67
Slc16a1	MCT1	Monocarboxylates	+	6.10
Slc16a2	MCT8	T3, T4	+	7.9
Slc19a1	RFT	N^5-Methyltetrahydrofolate	+	9.52
Slc19a2	ThTr1	Thiamine	+	4.9
Slc20a2	PiT-2	Pi, Na^+	+	8.57
Slco1a4	Oatp1a4	Digoxin, bile salts, organic anions, organic cations	++	6
Slco1a6	Oatp1a6	Organic anions	+	0
Slco1c1	Oatp1c1	T4, rT3, BSP	+	6.81
Slc22a3	Oct3	Organic cations	++	6.19
Slc22a5	OCTN2	L-Carnitine, organic cations	++	6.19
Slc22a7	Oat2	Organic anions	++	12.9
Slc22a8	Oat3	Organic anions	++	5.67
Slc23a1	SVCT1	L-Ascorbic acid	+	3.14
Slc23a2	SVCT2	L-Ascorbic acid	+	10.05
Slc27a5	FATP5	Long-chain fatty acids	+	5.38
Slc30a1	ZNT1	Zinc	+	1.71
Slc38a3	SNAT4	Neutral amino acids	+	8.9
Slc38a5	SNAT5	Neutral amino acids	+	4.29

+, significant expression; ++, strong expression; +++, very high expression.
[a] Relative expression level in the BBB.

TABLE 3
Slc genes with highest expression values ($E \geq 16$) in the choroid plexus (CP)

Gene Symbol	Protein Name	Substrates	CP Expression Factor	Average Brain Expression Factor
Slc2a12	GLUT12	Glucose	20	11
Slc4a2	AE2	Cl^-, HCO_3^-	20	5.8
Slc4a10	NCBE	Na^+, Cl^-, HCO_3^-	16	8.5
Slc5a3	SMIT	*Myo*-inositol	20	6.1
Slc6a20	SIT1	Imino acids	16	4.5
Slc7a4	CAT-4	Unknown	16	11
Slc7a6	y^+LAT2	Large, neutral L-amino acids and cationic amino acids	16	14
Slc12a2	NKCC1	Sodium, potassium, chloride	16	5.4
Slc13a4	NaS2	Sulfate	20	7.1
Slc16a2	MCT8	T3, T4	20	8
Slc19a1	RFT	N^5-Methyltetrahydrofolate	16	9.6
Slco1c1	Oatp1c1	T4, rT3, BSP	20	6.9
Slc22a17	BOIT	Unknown	20	16
Slc23a2	SVCT2	L-Ascorbic acid	20	10
Slc24a5	NCKX5	Na^+, Ca^{2+}	16	1.8
Slc25a3	PiC	Phosphate	16	12
Slc25a4	AAC1	ADP, ATP	16	20
Slc25a5	AAC2	ADP, ATP	16	12
Slc25a11	OGC	Oxoglutarate, malate	16	12
Slc25a12	ACG1	Aspartate, glutamate	16	17
Slc25a17	ANC1	ATP	16	8
Slc26a11		Sulfate	16	0.76
Slc27a1	FATP1	Long-chain fatty acids	16	11
Slc29a4	PMAT	Biogenic amines, adenosine	20	10
Slc31a1	Ctr1	Copper	16	7.7
Slc38a3	SNAT4	System A amino acids	20	8.9
Slc39a12		Zinc	16	2.1

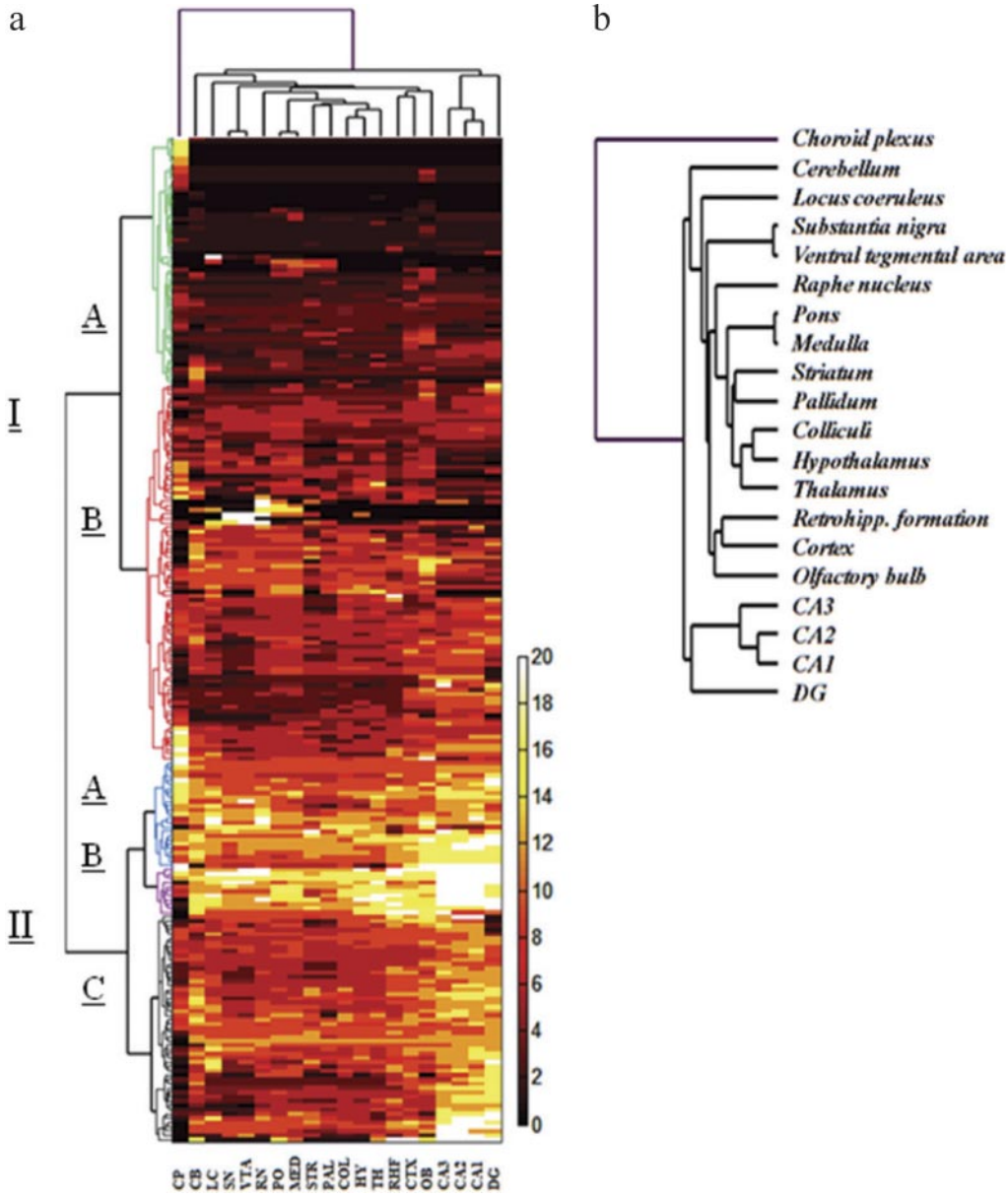

Fig. 7. Unsupervised hierarchical cluster analysis (UHCA) of *Slc* gene expression across the brain. Clustergram shown in a demonstrates results of UHCA of E values for *Slc* genes. UHCA produced two major clusters (labeled I and II, left), divided into five subclusters (dendrogram is color-coded for ease of identification). Label bar at the right of clustergram indicates the range of color-coded expression factor values presented in the heat map (from 0 to 20). In b, a magnified image of the dendrogram of clustered brain regions [shown as x-axis labels (a)] is shown. OB, olfactory bulb; CTX, cerebral cortex; PAL, pallidum; STR, striatum; DG, dentate gyrus; CA3, CA3 hippocampal field; CA2, CA2 hippocampal field; CA1, CA1 hippocampal field; RHF, retrohippocampal formation; CP, choroid plexus; T, thalamus; HY, hypothalamus; COL, colliculi; SN, substantia nigra; VTA, ventral tegmental area; LC, locus coeruleus; R, raphe; P, pons; MED, medulla; CB, cerebellum.

Across the brain, the average expression factor for the majority of *Slc* genes was low to moderate ($0 < \hat{E} < 10$), suggesting that many genes are either expressed at low levels throughout the brain or localized to a few brain areas. However, 39 *Slc* genes showed relatively high average expression factor values ($\hat{E} \geq 10$). Nine isoforms within the Slc25 mitochondrial carrier family are represented in this category, and four of them (*Slc25a1*, *Slc25a4*, *Slc25a12*, *Slc25a23*) are expressed at the highest level among all genes evaluated in this analysis. The abundant expression and wide distribution of Slc25 mitochondrial transporters across the brain is consistent with the brain's high energy demand, which consumes 25% of total body energy (Clark and Sokoloff, 1999). Located in the inner membrane of mitochondria, these proteins transport ADP/ATP and tricarboxylic acid cycle intermediates and are essential for ATP production and mitochondrial energy metabolism, an activity that fuels all basic and higher order cellular activities (Palmieri, 2004). Other highly expressed genes include transporters for nutrients, ions, and neurotransmitters (Table 1). These findings, together with the functional categorization of the 252 *Slc* genes present in the brain (Fig. 1b), suggest that Slc transporters play crucial roles in energy metabolism, nutrient supply, and neurotransmitter regulation in the brain.

The mammalian brain is anatomically complex, containing diverse cell types and distinct microstructures. These microstructures are associated with unique functional tasks and are specifically targeted by disease processes. Previous histological studies have only mapped the expression of a limited number of *Slc* genes in brain microstructures. In this study, we systematically and quantitatively analyzed the spatial and cellular distribution of 307 *Slc* genes in 20 anatomically comprehensive brain regions. Our analysis revealed complex and diverse expression patterns for the *Slc* genes (Figs. 3–6; Supplemental Figs. 1–4), suggesting important and diverse roles for this gene superfamily in the brain. Moreover, the identification of highly localized patterns and cell type-specific expression of cer-

tain *Slc* genes may provide important clues to their physiological functions within various neurochemical networks. For example, our study found that the low-affinity, high-capacity *CTL1* (*Slc44a1*), a novel and less characterized Slc transporter (O'Regan et al., 2000), is uniquely enriched in oligodendroglial cells (Fig. 6b). In contrast, the Na^+-dependent, high-affinity choline transporter 1 (*Slc5a7*) is known to be mainly expressed in cholinergic neurons, where it plays a critical role in sustaining synaptic cholinergic signaling (Bazalakova and Blakely, 2006). The distinct cellular distribution of *CTL1* suggests a fundamentally different role of this transporter in the brain. Because choline is also an essential precursor of membrane lipids (e.g., phosphatidylcholine, shingomylin) (Michel et al., 2006), CTL1 may function in the synthesis of biomembranes (including the myelin sheath) in oligodendroglial cells.

An important contribution of our study is the annotation of *Slc* gene expression at the BBB and choroid plexus, two important barriers that protect the brain from circulating xenobiotics and blood-borne pathogens. Several studies have attempted to characterize the gene expression profiles at the BBB using microarray or polymerase chain reaction-based serial analysis of gene expression approaches (Li et al., 2001; Enerson and Drewes, 2006). This study is the first where BBB expression of the *Slc* genes is systematically analyzed using ISH histological data. Here, we clearly identified 36 *Slc* genes expressed at the BBB, including many novel transcripts in addition to genes with known localization in this structure. Compared with the large number (202–233) of *Slc* genes identified in the choroid plexus and other brain subdivisions (Fig. 2), this number is relatively small, suggesting that our method is not sensitive enough to detect genes with relatively low expression at the BBB. Consistent with the role of the BBB in supplying essential nutrients to the brain, ~70% of the 36 *Slc* genes found at the BBB is involved in the transport of nutrients, vitamins, hormones, and trace metals (Table 2). On the other hand, genes involved in electrolyte transport and ATP production are well represented at the choroid plexus, consistent with its role in CSF production (Table 3). It is interesting that a few genes, including the thyroid hormone transporters *Slc16a2* and *Slco1c1*, the sulfate transporter *Slc13a4*, the reduced folate transporter *Slc19a1*, the L-ascorbic acid transporter *Slc23a2*, and the system A amino acid transporter *Slc38a3*, are coexpressed at high levels at both the BBB and the choroid plexus. These genes may play coordinated roles at the two blood-CNS interfaces to regulate brain homeostasis of nutrients and hormones.

Unsupervised, two-way hierarchical cluster analysis revealed that *Slc* gene expression patterns are associated with the neuroanatomical organization of the brain. In general, anatomically adjacent and functionally related structures share overlapping *Slc* expression profiles (Fig. 7b). It is interesting that marked enrichment of *Slc* genes was observed in the hippocampal areas (dentate gyrus, fields CA1, CA2, and CA3) in cluster II (Fig. 7; Supplemental Figs. 3–4). The highly expressed genes in the hippocampus include many mitochondrial carriers in the Slc25 family (*Slc25a1*, *Slc25a5*, *Slc25a11*, *Slc25a12*, *Slc25a16*, *Slc25a23*, *Slc25a27*, *Slc25a36*) and Golgi nucleoside-sugar transporters in the Slc35 family (*Slc35a1*, *Slc35a4*, *Slc35b1*, *Slc35b2*, *Slc35b3*, *Slc35e2*), which may suggest high volume of energy consumption and protein processing activities in this area.

In conclusion, we have identified the major Slc transporters expressed in defined brain structures and revealed the complex expression patterns represented by this gene superfamily. These studies will ultimately serve as a helpful resource for delineating the roles of *Slc* genes in the mammalian brain.

Acknowledgments

We thank Dr. Michael Hawrylycz for assistance in bioinformatic analysis and critical reading of the manuscript.

References

Allen DD and Geldenhuys WJ (2006) Molecular modeling of blood-brain barrier nutrient transporters: in silico basis for evaluation of potential drug delivery to the central nervous system. *Life Sci* **78:**1029–1033.

Arriza JL, Eliasof S, Kavanaugh MP, and Amara SG (1997) Excitatory amino acid transporter 5, a retinal glutamate transporter coupled to a chloride conductance. *Proc Natl Acad Sci U S A* **94:**4155–4160.

Bazalakova MH and Blakely RD (2006) The high-affinity choline transporter: a critical protein for sustaining cholinergic signaling as revealed in studies of genetically altered mice. *Handb Exp Pharmacol* **175:**525–544.

Beart PM and O'Shea RD (2007) Transporters for L-glutamate: an update on their molecular pharmacology and pathological involvement. *Br J Pharmacol* **150:**5–17.

Bhattacharjee Y (2006) Neuroscience: "Google of the brain": atlas maps brain's genetic activity. *Science* **313:**1879.

Blakely RD, De Felice LJ, and Hartzell HC (1994) Molecular physiology of norepinephrine and serotonin transporters. *J Exp Biol* **196:**263–281.

Clark DD and Sokoloff L (1999) in *Basic Neurochemistry: Molecular, Cellular and Medical Aspects* (Siegel GJ, Agranoff BW, Albers RW, Fisher SK, and Uhler MD eds) pp 637–670, Lippincott, Philadelphia, PA.

Dahlin A, Xia L, Kong W, Hevner R, and Wang J (2007) Expression and immunolocalization of the plasma membrane monoamine transporter in the brain. *Neuroscience* **146:**1193–1211.

Enerson BE and Drewes LR (2006) The rat blood-brain barrier transcriptome. *J Cereb Blood Flow Metab* **26:**959–973.

Engel K, Zhou M, and Wang J (2004) Identification and characterization of a novel monoamine transporter in the human brain. *J Biol Chem* **279:**50042–50049.

Enomoto A, Kimura H, Chairoungdua A, Shigeta Y, Jutabha P, Cha SH, Hosoyamada M, Takeda M, Sekine T, Igarashi T, et al. (2002) Molecular identification of a renal urate anion exchanger that regulates blood urate levels. *Nature* **417:**447–452.

Garland EM, Hahn MK, Ketch TP, Keller NR, Kim CH, Kim KS, Biaggioni I, Shannon JR, Blakely RD, and Robertson D (2002) Genetic basis of clinical catecholamine disorders. *Ann N Y Acad Sci* **971:**506–514.

Hagenbuch B and Meier PJ (1994) Molecular cloning, chromosomal localization, and functional characterization of a human liver Na^+/bile acid cotransporter. *J Clin Invest* **93:**1326–1331.

Hagenbuch B and Meier PJ (2004) Organic anion transporting polypeptides of the OATP/SLC21 family: phylogenetic classification as OATP/SLCO superfamily, new nomenclature and molecular/functional properties. *Pflugers Arch* **447:**653–665.

Haitina T, Lindblom J, Renström T, and Fredriksson R (2006) Fourteen novel human members of mitochondrial solute carrier family 25 (SLC25) widely expressed in the central nervous system. *Genomics* **88:**779–790.

Hediger MA, Romero MF, Peng JB, Rolfs A, Takanaga H, and Bruford EA (2004) The ABCs of solute carriers: physiological, pathological and therapeutic implications of human membrane transport proteins. *Pflugers Arch* **447:**465–468.

Kanai Y and Hediger MA (2004) The glutamate/neutral amino acid transporter family SLC1: molecular, physiological and pharmacological aspects. *Pflugers Arch* **447:**469–479.

Kong W, Engel K, and Wang J (2004) Mammalian nucleoside transporters. *Curr Drug Metab* **5:**63–84.

Kusuhara H and Sugiyama Y (2004) Efflux transport systems for organic anions and cations at the blood-CSF barrier. *Adv Drug Deliv Rev* **56:**1741–1763.

Lee G, Dallas S, Hong M, and Bendayan R (2001) Drug transporters in the central nervous system: brain barriers and brain parenchyma considerations. *Pharmacol Rev* **53:**569–596.

Lein ES, Hawrylycz MJ, Ao N, Ayres M, Bensinger A, Bernard A, Boe AF, Boguski MS, Brockway KS, Byrnes EJ, et al. (2007) Genome-wide atlas of gene expression in the adult mouse brain. *Nature* **445:**168–176.

Li JY, Boado RJ, and Pardridge WM (2001) Blood-brain barrier genomics. *J Cereb Blood Flow Metab* **21:**61–68.

Lindsey AE, Schneider K, Simmons DM, Baron R, Lee BS, and Kopito RR (1990) Functional expression and subcellular localization of an anion exchanger cloned from choroid plexus. *Proc Natl Acad Sci U S A* **87:**5278–5282.

Michel V, Yuan Z, Ramsubir S, and Bakovic M (2006) Choline transport for phospholipid synthesis. *Exp Biol Med (Maywood)* **231:**490–504.

Miller DS (2004) Confocal imaging of xenobiotic transport across the choroid plexus. *Adv Drug Deliv Rev* **56:**1811–1824.

O'Regan S, Traiffort E, Ruat M, Cha N, Compaore D, and Meunier FM (2000) An electric lobe suppressor for a yeast choline transport mutation belongs to a new family of transporter-like proteins. *Proc Natl Acad Sci U S A* **97:**1835–1840.

Palmieri F (2004) The mitochondrial transporter family (SLC25): physiological and pathological implications. *Pflugers Arch* **447:**689–709.
Pardridge WM (2007) Drug targeting to the brain. *Pharm Res* **24:**1733–1744.
Rothstein JD, Patel S, Regan MR, Haenggeli C, Huang YH, Bergles DE, Jin L, Dykes Hoberg M, Vidensky S, et al. (2005) Beta-lactam antibiotics offer neuroprotection by increasing glutamate transporter expression. *Nature* **433:**73–77.
Scott DA, Wang R, Kreman TM, Sheffield VC, and Karniski LP (1999) The Pendred syndrome gene encodes a chloride-iodide transport protein. *Nat Genet* **21:**440–443.
Simpson IA, Carruthers A, and Vannucci SJ (2007) Supply and demand in cerebral energy metabolism: the role of nutrient transporters. *J Cereb Blood Flow Metab* **27:**1766–1791.
Smith DE, Johanson CE, and Keep RF (2004) Peptide and peptide analog transport systems at the blood-CSF barrier. *Adv Drug Deliv Rev* **56:**1765–1791.
Sunkin SM and Hohmann JG (2007) Insights from spatially mapped gene expression in the mouse brain. *Hum Mol Genet* **16:**R209–R219.
Taylor KM, Morgan HE, Smart K, Zahari NM, Pumford S, Ellis IO, Robertson JF, and Nicholson RI (2007) The emerging role of the LIV-1 subfamily of zinc transporters in breast cancer. *Mol Med* **13:**396–406.
Tian G, Lai L, Guo H, Lin Y, Butchbach ME, Chang Y, and Lin CL (2007) Translational control of glial glutamate transporter EAAT2 expression. *J Biol Chem* **282:**1727–1737.
Torres GE, Gainetdinov RR, and Caron MG (2003) Plasma membrane monoamine transporters: structure, regulation and function. *Nat Rev Neurosci* **4:**13–25.
Vincourt JB, Jullien D, Amalric F, and Girard JP (2003) Molecular and functional characterization of SLC26A11, a sodium-independent sulfate transporter from high endothelial venules. *FASEB J* **17:**890–892.

Address correspondence to: Joanne Wang, Department of Pharmaceutics, University of Washington, H272J Health Sciences Building, Seattle, WA 98195. E-mail: jowang@u.washington.edu